

# Study of magnetic environment for neutron spin filters using polarized $^3\text{He}$ at J-PARC and JRR-3

Shusuke TAKADA<sup>1,2</sup>, Masaki FUJITA<sup>1</sup>, Yu Goto<sup>3,2</sup>, Takashi HONDA<sup>4</sup>, Kazutaka IKEDA<sup>4</sup>, Yoichi IKEDA<sup>1</sup>, Takashi Ino<sup>4</sup>, Koji KANEKO<sup>2</sup>, Ryuji KOBAYASHI<sup>5,2</sup>, Manabu OKAWARA<sup>1</sup>, Takayuki OKU<sup>2,5</sup>, Takuya OKUDAIRA<sup>3,2</sup>, Toshiya OTOMO<sup>4,5</sup> and Shingo TAKAHASHI<sup>5,2</sup>

<sup>1</sup>*Institute for Materials Research, Tohoku University, 2-1-1 Katahira, Aoba, Sendai, Miyagi, 980-8577, Japan*

<sup>2</sup>*J-PARC Center, Japan Atomic Energy Agency, 2-1 Shirakata, Tokai, Ibaraki, 319-1195, Japan*

<sup>3</sup>*Department of Physics, Nagoya University, Chikusa, Nagoya, Aichi, 464-8602, Japan*

<sup>4</sup>*Institute of Materials Structure Science, High Energy Accelerator Research Organization, 1-1 Oho, Tsukuba, Ibaraki, 305-0801, Japan*

<sup>5</sup>*Graduate School of Science and Engineering, Ibaraki University, 2-1-1 Bunkyo, Mito, Ibaraki, 310-8512, Japan*

*E-mail: shusuke.takada.d7@tohoku.ac.jp*

(Received January 5, 2023)

A neutron spin filter using polarized  $^3\text{He}$  is suitable for polarizing high-energy neutrons from meV to eV and is being developed at the J-PARC center. This device is utilized at a high temperature (200°C) and a low magnetic field (1 mT), however, homogeneity of a magnetic field is critical for maintaining the  $^3\text{He}$  polarization. We calculated the magnetic field gradient of solenoid coils intended for use in several neutron beamlines at J-PARC and JRR-3 using magnetic field simulations based on the finite element method. The field gradient is expected to be better than  $10^{-4} \text{ cm}^{-1}$ , which value implies that the neutron polarizer can be installed in a limited experimental space in the neutron beamlines.

**KEYWORDS:** neutron polarization, spin filter, Spin Exchange Optical Pumping method, finite element method

## 1. Introduction

High energy polarized neutron beams are desired in neutron scattering experiments and spin physics research [1–7]. A helium-3 ( $^3\text{He}$ ) spin filter is a polarization device suitable for neutrons with energies from meV to eV. The principle of neutron polarization using the  $^3\text{He}$  spin filter is based on the fact that the absorption cross-section of polarized  $^3\text{He}$  nuclei varies extremely depending on the spin of the incident neutron. In the 2000s, the  $^3\text{He}$  spin filter polarization of over 80% was obtained by the Spin Exchange Optical Pumping (SEOP) method using a glass cell encapsulating  $^3\text{He}$  gas, N<sub>2</sub> gas and a hybrid of two alkali metals, rubidium (Rb) and potassium (K) at a magnetic field of 1 mT and a temperature of around 200°C [8]. The SEOP method does not require cryogenic temperatures and high magnetic fields, enabling compact polarization systems, which can be installed in the limited experimental space of existing beamlines. However, the relaxation time of the  $^3\text{He}$  polarization is sensitive to an inhomogeneous magnetic field [9].

Installations of the  $^3\text{He}$  spin filters are planned in the neutron beamlines of Japan Proton Accelerator Research Complex (J-PARC) and Japan Research Reactor-3 (JRR-3). We report on designs of the  $^3\text{He}$  spin filter with sufficiently high homogeneity of the magnetic field obtained by using field simulation software based on the finite element method.



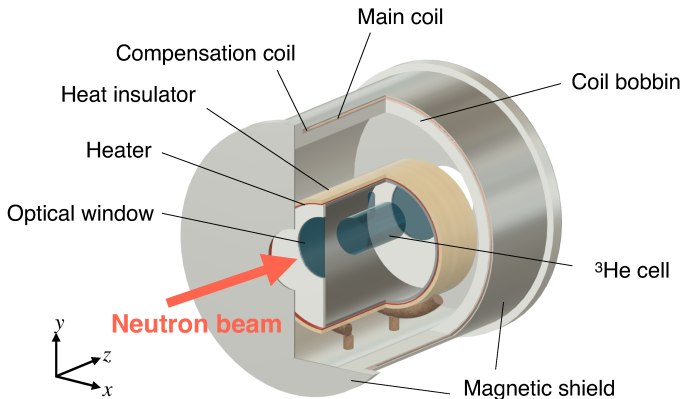


**Fig. 1.** A schematic of the  ${}^3\text{He}$  spin filter. The  ${}^3\text{He}$  spin filter consists of the  ${}^3\text{He}$  cell, the optical window, the coil bobbin, the main coil, the compensation coils, the heater, the heat insulator, and the magnetic shields. The cell and the optical window are made of boron-free material to transmit not only an infrared laser but also a neutron beam.

## 2. Polarization system and neutron beamline

In the SEOP method, the spin polarization of electrons produced in the alkali metal atoms by irradiating circular polarized infrared laser is transferred to  ${}^3\text{He}$  nuclei via the hyperfine interaction. A polarization system based on the SEOP consists of the  ${}^3\text{He}$  spin filter and an optical system, which are installed in a laser shield box. A structure of the  ${}^3\text{He}$  spin filter is shown in Fig. 1. It is composed of a  ${}^3\text{He}$  cell, a heater, a heat insulator, a coil bobbin, a solenoid type of the main coil, compensation coils, and magnetic shields from the inside out. The  $z$ -axis of Cartesian coordinates is defined as the long axis of the solenoid main coil. The  ${}^3\text{He}$  cell, in which a size of  $\phi 30\text{ mm} \times 50\text{ mm}$  is optimized for thermal neutrons, is placed at the center of the main coil. The cell is made of boron-free aluminosilicate glass (GE180) which is widely used for the glass cell of the  ${}^3\text{He}$  spin filter because of the low permeability of the  ${}^3\text{He}$  gas and a small wall relaxation effect. It is filled with  $\text{N}_2$  (0.1 atm),  $\text{Rb}$ , and  $\text{K}$  in addition to the  ${}^3\text{He}$  gas (3 atm). The heater and the heat insulator are used for keeping the temperature around  $200^\circ\text{C}$  to be evaporated the alkali metals. A magnitude of a magnetic field is applied 1 mT by the main coil. The magnetic field homogeneity is improved by the compensation coils. Both the main coil and the compensation coils are two-layered. Copper wire of  $\phi 1\text{ mm}$  in diameter is used for these coils, which are wound onto the coil bobbin without gaps. The magnetic shield, consisting of a sheet and boards, is made of permalloy to absorb the stray magnetic field. The boards have  $\phi 50\text{ mm}$  size of holes to accept a neutron beam. The thickness of the magnetic shield is 0.2 mm.

*Ex-situ* and *in-situ* methods are used for the  ${}^3\text{He}$  spin filters, depending on the purpose of use in a neutron beam experiment. The *in-situ* method has the advantage that the  ${}^3\text{He}$  polarization does not relax during the experiment because the neutron beam is irradiated while performing the SEOP. The *ex-situ* method has the advantage of saving even more space than the *in-situ* method, although the polarization of  ${}^3\text{He}$  decreases during the experiment. The *in-situ* and *ex-situ* methods are suitable for experiments that are conducted over a period of days to weeks, and for short-duration experiments, respectively. The two types of the  ${}^3\text{He}$  spin filters are planned to use at the neutron beamlines of beamline 21 (BL21) NOVA [10, 11] at Material and Life science facility (MLF) in J-PARC, and beamline 6G TOPAN [12] in JRR-3. NOVA aims to research magnetic structural changes or pair correlation in hydrogen-induced physical properties, hydrogen storage materials, or amorphous compounds by using the world-highest intensity of a pulsed neutron beam of the J-PARC MLF. TOPAN aims for high-resolution measurement of magnetic excitations in strongly correlated electron systems

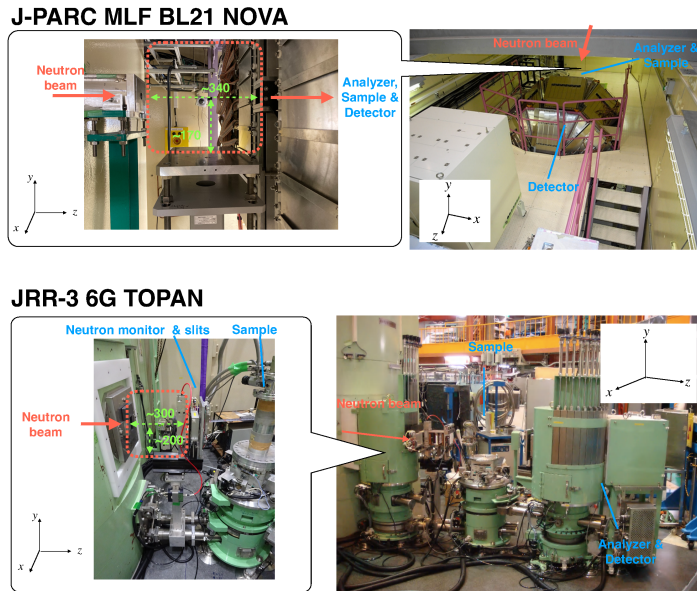


**Fig. 2.** Photographs of NOVA (top) and TOPAN (bottom). Dotted squares denote the installed positions of the  ${}^3\text{He}$  spin filters.

using polarized neutrons. The JRR-3 has been utilized as a top-level high-performance research reactor worldwide for beam experiments and neutron irradiation, and this facility has just returned from a prolonged shutdown. Figure 2 shows photographs of the space planned for the spin filter installation in NOVA and TOPAN. Each beamline has a space of 30 cm square upstream from a sample position. The *ex-situ* and *in-situ* spin filters will be installed for NOVA and TOPAN, respectively.

### 3. Field homogeneity of the coil

The homogeneity of the magnetic field strongly depends on the diameter and length of the coil, and the number of turns of the compensation coils. Magnetic field simulations of the coils based on the finite element method were performed to design the optimal coil for NOVA and TOPAN beamlines. Figure 3 shows a two-dimensional ( $x$ - $z$ ) distribution of the field gradient of the coil. Contour lines refer to the gradient of the magnetic field. The field gradient is defined as

$$\frac{|B_{\perp}|}{|B_z|} = \frac{\sqrt{|\nabla B_x|^2 + |\nabla B_y|^2}}{|B_z|}, \quad (1)$$

where  $B_x$ ,  $B_y$ ,  $B_z$  are  $x$ ,  $y$  and  $z$  components of the magnetic field [13]. The dotted line near the distribution's origin means a  ${}^3\text{He}$  cell region. The inhomogeneity is calculated from the volume-weighted average of the magnetic field gradients in the  ${}^3\text{He}$  cell region, which size was mentioned in Sec. 2.

The performance of the coil is evaluated by a relaxation time of the  ${}^3\text{He}$  polarization, which depends on the field inhomogeneity. A time ( $t$ ) variation of the polarization ( $P_{{}^3\text{He}}$ ) is explained as

$$P_{{}^3\text{He}} = P_0 \exp\left(-\frac{t}{T_1}\right),$$

where  $P_0$  is a magnitude of an initial polarization,  $T_1$  is the relaxation time. Here, the relaxation time

$T_1$  is the sum of the four components:

$$\frac{1}{T_1} = \frac{1}{T_1^{\text{gradient}}} + \frac{1}{T_1^{\text{dipole}}} + \frac{1}{T_1^{\text{impurity}}} + \frac{1}{T_1^{\text{wall}}},$$

where  $T_1^{\text{gradient}}$ ,  $T_1^{\text{dipole}}$ ,  $T_1^{\text{impurity}}$  and  $T_1^{\text{wall}}$  are components for the field inhomogeneity, a dipole-dipole interaction of  ${}^3\text{He}$  nuclei, an interaction with impurities and an interaction with a wall molecule, respectively [9]. Notably, the component of the field inhomogeneity is expressed as

$$\frac{1}{T_1^{\text{gradient}}} = \frac{6700}{p} \left( \frac{|\nabla B_x|^2 + |\nabla B_y|^2}{B_z^2} \right) \text{ h}^{-1},$$

where  $p$  is a gas pressure of  ${}^3\text{He}$ . Here, the square of the field inhomogeneity  $(|\nabla B_x|^2 + |\nabla B_y|^2)/B_z^2$  is assigned the value calculated based on Fig. 3 and Eq. 1. The relaxation time  $T_1^{\text{gradient}}$  is preferable sufficiently longer than  $T_1^{\text{dipole}}$  which is approximately 200 h at the gas pressure 3 atm. Therefore, the desired value of  $\sqrt{|\nabla B_x|^2 + |\nabla B_y|^2}/B_z$  is approximately  $10^{-4} \text{ cm}^{-1}$ , in which case  $T_1^{\text{gradient}}$  is exceeded  $10^4$  h.

The relaxation time due to the field inhomogeneity was calculated for the different sizes of the coils. Figure 4 shows the coil radius dependence of the relaxation time  $T_1^{\text{gradient}}$ , with the number of turns of the compensation coils on the horizontal axis. The coil length was fixed to 180 mm. The maximum values of the relaxation time are independent of the coil radius. Since the heat insulator and the heater are installed inside the main coil to keep the temperature around 200°C, the coil radius of 80 mm is appropriate. Figure 5 shows the coil length dependence of the relaxation time  $T_1^{\text{gradient}}$ , with the number of turns of the compensation coils on the horizontal axis. The coil radius was fixed to 100 mm. The number of turns was set to 90% of the coil length in mm, since the actual copper wire spacing will have gaps due to the twisting of the copper wire. The longer the coil length, the improved homogeneity of the magnetic field and the maximum relaxation time. Since the *ex-situ* spin filter will be installed in NOVA, the optimal coil length is 300 mm, which corresponds to the length of the space shown in Fig. 2. For the *in-situ* spin filter to be used in TOPAN, the coil length of 180 mm is appropriate because optical mirrors and guide coils for neutron spin are also installed within the installation space. The relaxation times  $T_1^{\text{gradient}}$  are expected to be greater than  $10^4$  h by adjusting the number of turns of the compensation coils.

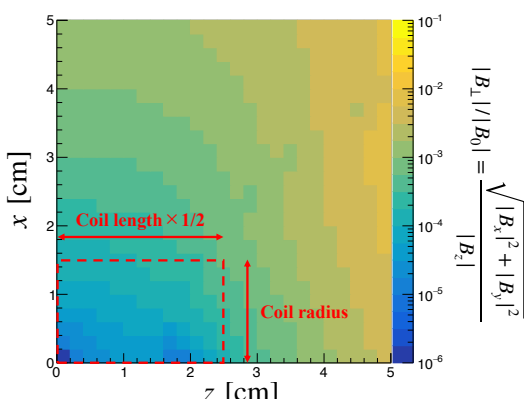


**Fig. 3.** A two-dimensional ( $x$ - $z$ ) distribution of a field gradient of the coil. The dotted line shows the position of the  ${}^3\text{He}$  cell. The arrows show a half-length and a radius of the main coil, respectively.

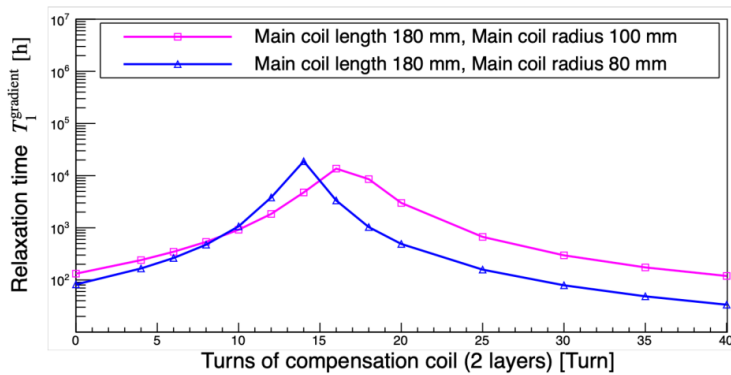


**Fig. 4.** A coil radius dependence of the relaxation time of  $^3\text{He}$  polarization. The horizontal axis shows the turns of compensation coils. The vertical axis shows the relaxation time. The filled triangles and the open squares were obtained from simulations for coil radii of 100 mm and 80 mm, respectively.

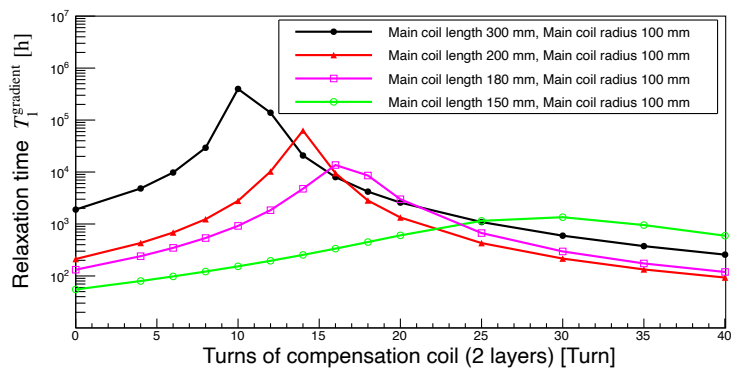


**Fig. 5.** A coil length dependence of the relaxation time of  $^3\text{He}$  polarization. The horizontal axis shows the turns of compensation coils. The vertical axis shows the relaxation time. The filled circles, the filled triangles, the open squares, and the open circles were obtained from simulations for coil lengths of 300 mm, 200 mm, 180 mm and 150 mm, respectively.

#### 4. Summary

The  $^3\text{He}$  spin filter is suitable devices for polarizing neutrons with energies from meV to eV. The coils with the high field homogeneity are required to achieve the high  $^3\text{He}$  polarization. The coils were designed for experiments at J-PARC BL21 NOVA and JRR-3 6G TOPAN. The expected relaxation time caused by the field inhomogeneity is more than  $10^4$  h, which is sufficiently longer than that due to the dipole-dipole interaction.

#### References

- [1] E. Babcock, S. Zahir, T. Tobias, S. Denis, S. Johann, F. Artem, M. Stefan, P. Patrick, R. Aurel, I. Alexander, J. Phys. Conf. Ser. **711** 012008 (2016).
- [2] I. Dhiman, R. Ziesche, T. Wang, H. Bilheux, L. Santodonato, X. Tong, C.Y. Jiang, I. Manke, W. Treimer, T. Chatterji, N. Kardjilov, Rev. Sci. Instrum. **88** 095103 (2017).
- [3] W.C. Chen, J.G. Barker, R. Jones, K.L. Krycka, S.M. Watson, C. Gagnon, T. Perevozchivoka, P. Butler, T.R. Gentile, J. Phys. Conf. Ser. **862** 012004 (2017).

- [4] E. Lelievre-Berna, *Phys. B* **397** 162 (2007).
- [5] W.T.H. Lee, T. D' Adam, *Neutron News* **27** 35 (2016).
- [6] C.J. Beecham, S. Boag, C.D. Frost, T.J. McKetterick, J.R. Stewart, K.H. Andersen, P.M. Bentley, D. Julian, *Physica B* **406** 2429 (2011).
- [7] T. Okudaira, T. Oku, T. Ino, H. Hayashida, H. Kira, K. Sakai, K. Hiroi, S. Takahashi, K. Aizawa, H. Endo, S. Endo, M. Hino, K. Hirota, T. Honda, K. Ikeda, K. Kakurai, W. Kambara, M. Kitaguchi, T. Oda, H. Ohshita, T. Otomo, H.M. Shimizu, T. Shinohara, J. Suzuki, T. Yamamoto, *Nucl. Instrum. Methods Phys. Res. A* **977** 164301 (2020).
- [8] E. Babcock, I. Nelson, S. Kadlecak, B. Driehuys, L.W. Anderson, F.W. Hersman, T.G. Walker, *Phys. Rev. Lett.* **91** 123003 (2003).
- [9] J.W. McIver, R. Erwin, W.C. Chen, T.R. Gentile, *Rev. Sci. Instrum.* **80** 063905 (2009).
- [10] K. Nakajima, Y. Kawakita, S. Itoh, J. Abe, K. Aizawa, H. Aoki, H. Endo, M. Fujita, K. Funakoshi, W. Gong, M. Harada, S. Harjo, T. Hattori, M. Hino, T. Honda, A. Hoshikawa, K. Ikeda, T. Ino, T. Ishigaki, Y. Ishikawa, H. Iwase, T. Kai, R. Kajimoto, T. Kamiyama, N. Kaneko, D. Kawana, S.O. Kawamura, T. Kawasaki, A. Kimura, R. Kiyanagi, K. Kojima, K. Kusaka, S. Lee, S. Machida, T. Masuda, K. Mishima, K. Mitamura, M. Nakamura, S. Nakamura, A. Nakao, T. Oda, T. Ohhara, K. Ohishi, H. Ohshita, K. Oikawa, T. Otomo, A.S. Furukawa, K. Shibata, T. Shinohara, K. Soyama, J. Suzuki, K. Suzuya, A. Takahara, S. Takata, M. Takeda, Y. Toh, S. Torii, N. Torikai, N.L. Yamada, T. Yamada, D. Yamazaki, T. Yokoo, M. Yonemura, H. Yoshizawa, *Quantum Beam Sci.* **1** 9 (2017).
- [11] T. Otomo, K. Suzuya, M. Misawa, N. Kaneko, H. Ohshita, K. Ikeda, M. Tsubota, T. Seya, T. Fukunaga, K. Itoh, M. Sugiyama, K. Mori, Y. Kameda, T. Yamaguchi, K. Yoshida, K. Maruyama, Y. Kawakita, S. Shamoto, K. Kodama, S. Takata, S. Satoh, S. Muto, T. Ino, H.M. Shimizu, T. Kamiyama, S. Ikeda, S. Itoh, Y. Yasu, K. Nakayoshi, H. Sendai, S. Uno, M. Tanaka, K. Ueno, *KENS Rep.* **17** 28 (2011).
- [12] S. Funahashi, *Physica B Condens. Matter* **174** 470 (1991).
- [13] G.D. Cates, S.R. Schaefer, W. Happer, *Phys. Rev. A* **37** 2877 (1988).